

Exploring Diffusional Behaviour in Nanostructured Systems with Single Molecule Probes: From Nanoporous Materials to Living Cells

Christophe Jung, Jens Michaelis, Nadia Ruthardt, Christoph Bräuchle

Department für Chemie und Biochemie and Center for Nanoscience (CeNS), Ludwig-Maximilians-Universität München, Butenandtstrasse 11, Gerhard-Ertl-Gebäude, D-81377 München, Germany

Corresponding author:

Christoph Bräuchle

Department für Chemie und Biochemie

Ludwig-Maximilians-Universität München

E-Mail: Christoph.Braeuchle@cup.uni-muenchen.de

1. Introduction

Molecular movement in confined spaces is of broad scientific and technological importance in areas ranging from molecular sieving and membrane separation to active transport along intracellular networks. By viewing a movie of a single fluorescent dye molecule moving within the nanostructured channel system of a mesoporous silica host, we see incredible details of molecular motions, be they translation, rotation, trapping at specific sites, lateral motion between defect (“leaky”) channels or bouncing back from disordered regions, to mention only a few examples. In this way single molecule tracking experiments create a new quality of understanding the dynamics and interactions of molecules in nano- or mesoporous silica structures [1-6]. This is of high importance for many applications of these attractive nanomaterials, which have been used as hosts for numerous molecular and cluster-based catalysts [7], for molecular sieving and chromatography [8], for the stabilization of conducting nanowires [9-11], as a matrix for ultrasmall dye lasers [12] and for novel drug-delivery systems [13], to mention only some of them. In many of these cases, the complete characterization of the transport and of the dynamics of guest molecules in the channels is crucial for the successful functionality of these materials. They can be formed through cooperative self assembly of surfactants and framework building blocks [14] with widely tuneable properties like e.g. channel diameters (2-50 nm), topologies (hexagonal, cubic or lamellar) and functionalized walls.

In this article we will show how single molecules can be used to investigate nanoporous materials and that the methodology can be helpful in the design of nanoscopic devices with high control of molecular dynamics such as new silica-based drug delivery systems. We first present a unique combination of transmission electron microscopic (TEM) mapping and optical single molecule tracking experiments (SMT) (section 2). We will then show how single dye molecules can be used as nanoscale probes to map out the structure of different mesoporous silica materials with different phase topologies (section 3). This will be followed by the presentation of our analysis method applied on a typical single molecule trajectory (section 4). We will then discuss additional polarization dependent studies which reveal the orientational motion

simultaneously to the translational movement (section 5) as well as single molecule measurements with very high positioning accuracy down to the single channel limit (section 6). This will be followed by the discussion of the potential utilization of mesoporous nanoparticles with functionalized pore walls as novel drug delivery systems (section 7). Finally we show how synthetic viruses as further drug or gene delivery systems can be used and how their uptake and movement within a living cell can be observed and analyzed (section 8).

2. Correlation of Structural and Dynamic Properties Using TEM and SMT

Mesoporous structures are commonly characterized with diffraction and electron microscopy methods [15] and gas sorption techniques. The ensemble diffusion behaviour of small molecules has been examined with pulsed-field gradient NMR spectroscopy [16] and neutron scattering [17]. Here we are interested in techniques which give a more direct access to the real structure of the mesoporous host and to the dynamics on a single molecule basis and thus reveal structural and dynamic features which are not obscured by ensemble or statistical averaging as in conventional techniques.

High resolution transmission electron microscopy (TEM) offers a way to directly see the channel structure of a mesoporous host [18]. Fig. 1a shows an example of a high resolution TEM image of a thin film as M41S which exhibits a hexagonal phase (see sketch in Fig. 1b). The film was prepared by spin-coating a mixture of a silica precursor (TEOS: tetraethyl-ortho-silicate), a template (Brij56: Polyoxyethylene-10-cetylother) and the probe dye molecule (a terrylendiimide derivative (TDI) [19] in an acidic water-ethanol solution resulting in a thin film (< 100 nm) via evaporation-induced self-assembly [14]. It is quite clear that such an image of TEM gives us the landscape of the channels in which our dye molecule can move. Although the TEM image is an average over the thickness of the film (approx. 10 - 20 layers of channels) this is the most realistic picture we can get about the real structure of the host. The drawback, however, is that the size of such a high resolution TEM image is limited to about 200×200 nm and the film has to be very thin.

Structural details like channel diameters on the scale of a few nanometers cannot be directly imaged with optical methods. However, single molecule fluorescence microscopy can track the movement of individual dye molecules incorporated as guests into mesoporous silica thin films in an epifluorescence microscope equipped with a highly sensitive CCD camera in a wide-field imaging set-up [1, 2]. As the films were much thinner than the focal depth of the microscope objective used, the images contain data from molecules though the whole film height and from the surface of the sample. Series of 1,000 images were acquired with a temporal resolution of down to 100 ms per frame. In each movie frame, single molecules show up as bright spots on a dark background. Their positions were obtained by fitting theoretical diffraction patterns to the spots, with a positioning accuracy down to 15 nm. Single-molecule trajectories were then built up by tracking spots from frame to frame. Examples are shown in Fig. 1c.

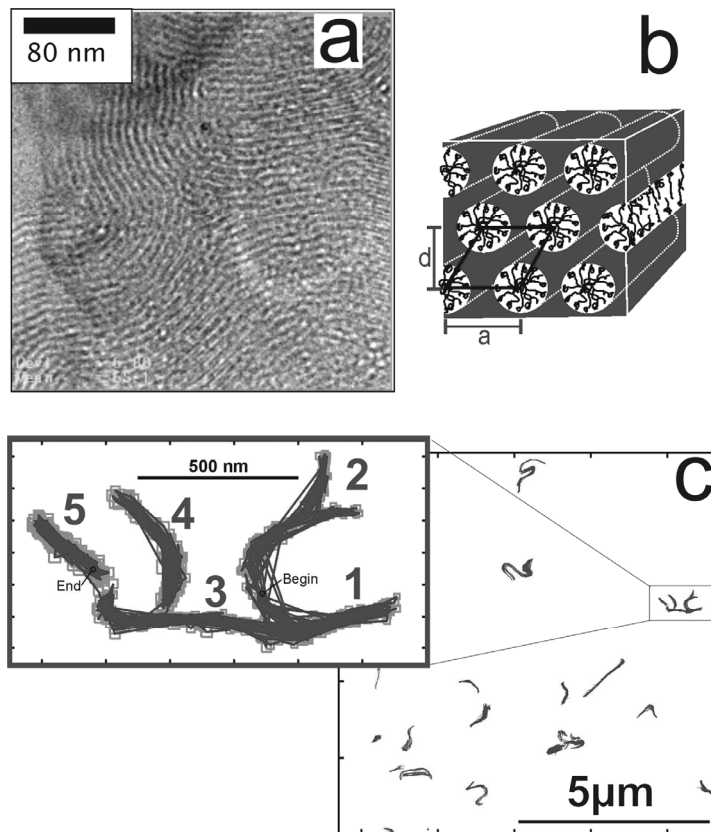


Fig. 1: **Sample system and single-molecule trajectories** a) High resolution TEM image gives the landscape of a channelar structure of a hexagonal mesoporous system. b) Schematic diagram of the hexagonal pore topology. c) SMT gives the trajectories of the movement of single molecules as guests in the nanoporous host. The enlarged inset shows the trajectory of a molecule which explores five different domains.

The trajectories show that the molecules in the hexagonal phase travel in a highly structured manner over distances of several μm during the acquisition time of the movie (500 s). The inset shows an enlargement of one of these trajectories. This molecule travels first along the C-shaped structure on the right (1) and after 65 s enters into the side-arm (2). Then, 100 s later, it passes into the linear structure at the bottom (3). After another 144 s, it enters region 4 and moves around there for 69 s before coming back to region 3. At the end it passes into region 5, where it moves back and forth for 109 s until the end of the movie (Movie S1 in supplementary material of ref. [1]). We note that the molecule apparently probes the domain boundaries in this process, by repeatedly ‘bouncing’ back from dead ends of the channel regions. This is one of the many striking examples that show how a single molecule seems to explore the structure of the host. We argue that such non-random diffusion, which is repeatedly seen in the hexagonal phase,

directly maps the alignment of the channels and the domain structure. Moreover, it seems that we “see” the structure of the host from the viewpoint of the molecule, i.e. we get information about the accessibility of the channels and the connectivity of the domains for the molecule in an unprecedented way, which is not possible with any other method. A proof, however, that the molecule really follows the channel system can only be given by a proper overlay of the structure of the channels as obtained by TEM with the trajectories of the single molecules as observed by SMT. Such a correlation can then clearly illuminate all the highly interesting aspects mentioned above, which can be summarized in one general question: how do structural elements correlate with and influence the dynamics of the molecules in the nanoporous channels? Because the molecular movement in the pore system is the most important and defining characteristic of nanoporous materials and its various applications, it is of high interest to learn about this behaviour as function of the local structure.

For the overlay of the optical and electron microscopic images we prepared a ca 50 nm thin spin-coated film directly onto the 30 nm thick Si_3N_4 membrane of the TEM sample holder [2]. Single polystyrene beads were incorporated into the film which can be imaged by TEM and optical microscopy. By first recording the trajectories with the optical widefield microscope and then measuring TEM images of the same sample region the correct correlation of both images could be achieved by overlapping the same pattern of the polystyrene beads. This tedious procedure is described in detail in ref. [2] and gives an overlay accuracy between 4 nm and 30 nm depending on the number of beads in the images. Fig. 2a shows the overlay of a single molecule trajectory with a high resolution ($\times 40,000$ magnification) TEM map. The latter was obtained from many high resolution TEM images (as shown in Fig. 1a) where adjacent square regions of $133 \text{ nm} \times 133 \text{ nm}$ make up the whole map. In each square region fast Fourier transformation (FFT) results in an FFT director which depicts the average orientation of the pores and the line thickness is a measure of the degree of structural order in this region. These directors are a good guide for the eye about the orientation of the channels and give an overview of the domain sizes.

Fig. 2a shows an example of a molecule faithfully following the pores and mapping out specific elements of the host structure (Movie 3 in supplementary material of ref. [2]). The perfect overlay of the S-shaped trajectory with the direction of the pore system is shown well by the FFT directors. In Fig. 2b a specific region of Fig. 2a is enlarged and shows the channel structure as well as the trajectories in more detail. In both figures the small boxes of the trajectory indicate the position accuracy of the molecular positions determined. These are in the range of 15-30 nm which means that the molecule's position can therefore be assigned not to a single channel, but to an ensemble of about 3-6 parallel channels. Furthermore, one should keep in mind that we are sampling diffusion at discrete points in time and space. Thus the connecting lines are just a method of visualizing the trajectories; they do not represent the molecules' exact path. The enlargement in Fig. 2b, however, clearly shows that the molecule in the upper part bounces back from the domain boundary with channels having different orientation as sketched in the inset of Fig. 2b. In the lower part of the trajectory, however, the molecule can find its way through along the main domain which guides the pathway of the S-

shaped trajectory. Many more structural elements such as the ones shown in Fig. 2c are found and could be correlated with the dynamic behaviour of single molecules.

In summary the combination of the two techniques provides the first direct proof that the molecular diffusion pathway through the pore system correlates with the pore orientation of the hexagonal structure. In addition, the influence of specific structural features of the host on the diffusion behaviour of the guest molecules can be clearly seen.

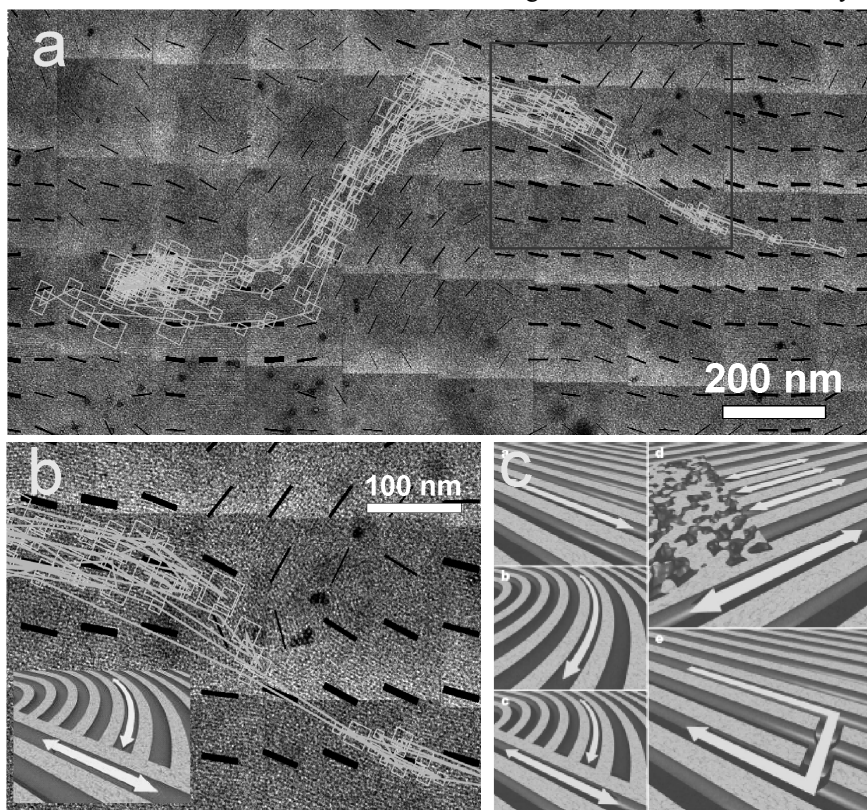


Fig. 2: **Molecular trajectories and structural elements in a hexagonal mesoporous silica film.** a) Overlay of an S-shaped trajectory of a single molecule with a transmission electron microscopy map. The molecule is exploring regions of parallel channels, strongly curved areas and domain boundaries indicated by the FFT directors (black bars). b) Enlarged area of a) showing part of the trajectory of the single molecule which bounces back repeatedly from a domain boundary formed by channels having different orientations as sketched in the inset. The small boxes in a) and b) depict the positioning accuracy. c) Sketches of structural elements and molecular movements found in hexagonal mesoporous silica films.

With this approach we can uncover, in unprecedented detail, how a single fluorescent dye molecule travels through linear or strongly curved sections of the hexagonal channel system, how it changes speed and how it bounces off a domain boundary with a different channel orientation. Furthermore, we can show how molecular travel is stopped at a less ordered region, or how lateral motions between ‘leaky’ channels allow a molecule to explore different parallel channels within an otherwise well-ordered periodic structure.

3. Phase Mixture

An interesting aspect of mesostructured silicas is that by varying the molar ratio between the surfactant and the silica oligomers of the precursor solution, materials with different mesopore topologies can be prepared. In this section we present the single molecule investigation of mesoporous silica films in which a hexagonal and a lamellar mesophases coexist [1]. We demonstrated that these topologies in fact strongly influence the diffusion of the single molecules inside the pores and the lamellas of the host [6].

Fig. 3a shows the first image of a Movie (Movie S5 in supplementary material of ref. [1]) showing single TDI molecules diffusing in a mixture of a hexagonal and of a mesoporous lamellar phase. Here, gaussian-shaped and doughnut-shaped patterns as fluorescence images of single molecules coexist within the same region. A gaussian-shaped pattern is obtained for a molecule which rotates, whereas a doughnut-shaped pattern is assigned to a single molecule with its transition dipole (here, the long molecular axis of TDI) aligned along the optical axis of the microscope [20]. In the present case, this means that molecules in the lamellar phase are oriented perpendicular to the glass substrate and thus normal to the silica planes of the lamellar phase. The inset shows magnified images of the two molecules indicated by the arrows. Overall, we can distinguish four populations of molecules on the basis of their different diffraction patterns and diffusive behaviour in the movie of this phase mixture. The first type comprises molecules with gaussian-shaped spots, which are diffusing along distinct trajectories over a large range of 1–5 μm . The second type has characteristic doughnut-shaped diffraction patterns exhibiting unstructured diffusion in two dimensions. Another, much smaller population consists of molecules that diffuse much faster, without showing any particular structure in their trajectories. An additional important observation is that multiple changes between these three types of mobility were observed for many of the molecules. Finally, we observed very few immobile molecules.

In accordance with the observations in the pure phases we assign the structured trajectories of population 1 to molecules in regions with a hexagonal arrangement of pores, and the molecules with doughnut-shaped patterns of population 2 that are diffusing very slowly and randomly, to other regions with lamellar structure, present simultaneously within this sample. The diffusion behaviour of the two remaining populations is not correlated with the pore topologies in the sample. In fact, the fast molecules of population 3, with unstructured trajectories, could be removed by washing the surface of the sample with water, clearly indicating that the molecules were on the surface of the film.

The diffusion behaviour in this phase mixture fits remarkably well with that in the pure phases. Interestingly, some molecules can be seen migrating between the phases. This observation demonstrates clearly that the two phases are actually interconnected.

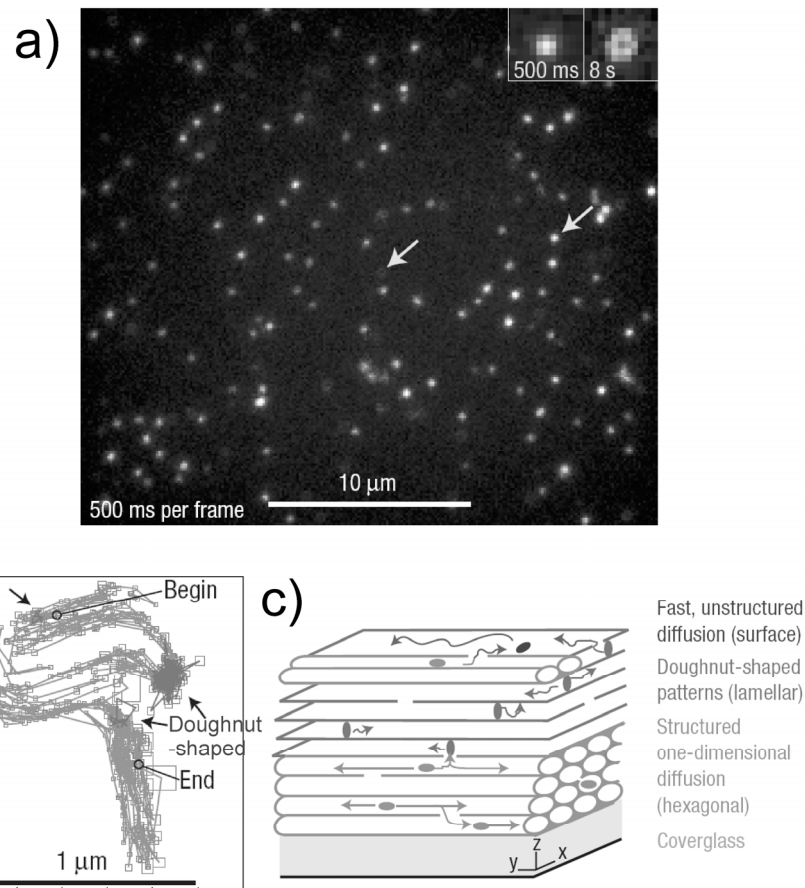


Fig. 3: Diffusion of single molecules in the phase mixture. a) A single-molecule image of the phase mixture contains both gaussian- and doughnut-shaped diffraction patterns. Magnified images of the molecules indicated by the arrows are shown in the upper right corner. b) An individual molecule undergoing several changes between the hexagonal (blue parts) and the lamellar phases (green parts, indicated by the arrows). c) Schematic diagram of the diverse diffusion modes observed in the wide-field movies of the phase mixture.

A specific example is shown in Fig. 3b. Again, as in the pure hexagonal phase, the shape of the trajectory explored by the gaussian pattern clearly reflects the underlying pore structure of the hexagonal phase. This molecule changed three times from a gaussian spot to a doughnut and back with different residence times in each phase (see Movie S6 in supplementary material of ref. [1]). Such switching phenomena clearly show that the two phases are actually connected, probably via structural defects at the phase boundaries. Interestingly, we also observed other cases where the molecule switches several times from a gaussian to a doughnut-shaped pattern at exactly the same position,

showing that molecules sometimes pass repeatedly through the same defect region between phases.

To conclude, we have shown that the structure of the trajectories, the diffusivities and the orientation of single molecules are clearly distinctive for molecules travelling in the lamellar and the hexagonal mesophases. A general schematic diagram of the different phases present in the film and the migration within as well as between the phases is shown in Fig. 3c.

4. Heterogeneous Dynamics of a Single Molecule

This section is a demonstration of how the data obtained by SMT can be evaluated. In particular, we will see that the detailed analysis of a typical single molecule trajectory provides information about the heterogeneities of the silica host nanostructure.

Fig. 4 shows such a case for an individual molecule of population 1 in the phase mixture of section 3. The molecule in Fig. 4a moves in a distinct structure and explores at least three different domains, indicated as A, B and C (Movie S8 in supplementary material of ref. [1]). Similar to the molecule in the pure hexagonal phase, this trajectory gives a lucid picture not only of the channel structure but also of the connectivity and accessibility of channels between different domains.

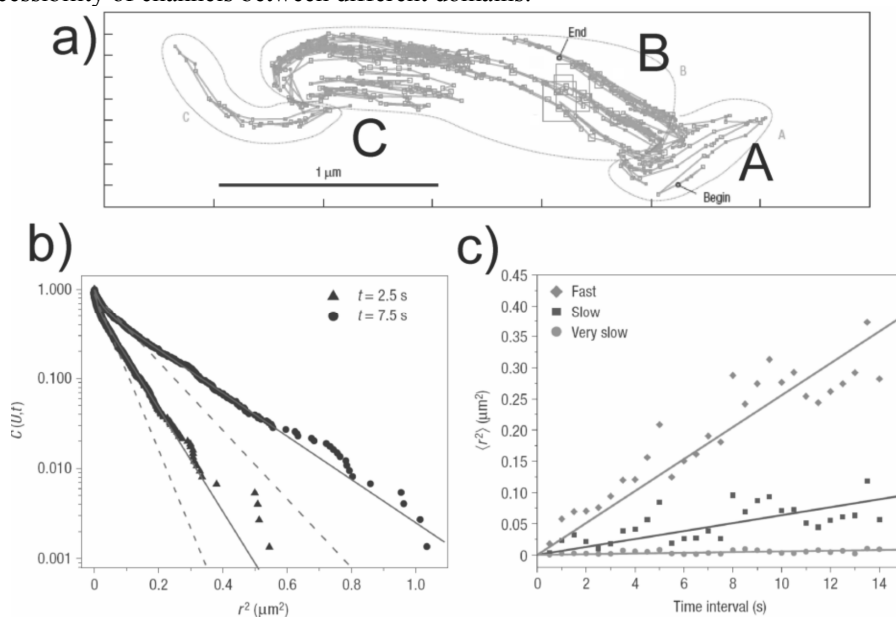


Fig. 4: Diffusion analysis of an individual trajectory in the hexagonal phase of the mixture. a) Trajectory of a molecule diffusing in a structured manner in different domains (A, B, C). b) Plot of cumulative probability of the square displacement r^2 for two sample time intervals ($t=2.5$ s, 7.5 s). Mono-exponential fits (dashed line) and tri-exponential fits (full line) are given. c) Plot of the mean-square displacement $\langle r^2 \rangle$ against the time intervals. Fits according to $\langle r^2 \rangle = 2Dt$ for the three different characteristic $\langle r^2 \rangle$ distributions.

For the molecule moving in this structure, a detailed analysis of the diffusion

behaviour was done by plotting the cumulative probability $P(r^2, t)$ of the squared displacements r^2 for different time lags t . [21, 22] Analyzing probability distributions instead of histograms allows for a more precise analysis, avoiding loss of information due to binning of the histogram. The data were fitted with multi-exponential decay functions:

$$P(r^2, t) = \sum_{i=1}^n a_i \exp\left(-\frac{r^2}{\langle r_i(t)^2 \rangle}\right) \quad (1)$$

where a_i is the amplitude of the different components and $\langle r_i(t)^2 \rangle$ the characteristic value for the mean-square displacement.

Regular diffusion should result in a mono-exponential decay ($n = 1$), giving a characteristic value for the mean-square displacement $\langle r_1(t)^2 \rangle$ for each time lag t . Fig. 4b shows the cumulative probability distributions for two sample time intervals ($t = 2.5$ s and 7.5 s). Here, the data cannot be fitted with a mono-exponential decay function (dashed lines in Fig. 4b). Tri-exponential decay functions ($n = 3$) were found to describe the data best (solid lines), giving three characteristic $\langle r_i(t)^2 \rangle$ values for each time lag. These values are plotted against time in Fig. 4c. We fitted the three different sets of $\langle r_i(t)^2 \rangle$ values with the Einstein–Smoluchowski equation for random diffusion in one dimension

$$\langle r_i(t)^2 \rangle = 2D_i t \quad (2)$$

giving values of $D_1 = 1.3 \times 10^{-2} \mu\text{m}^2 \text{s}^{-1}$, $D_2 = 3.2 \times 10^{-3} \mu\text{m}^2 \text{s}^{-1}$ and $D_3 = 2.8 \times 10^{-4} \mu\text{m}^2 \text{s}^{-1}$. These large differences imply that the molecule is diffusing in at least three kinds of environments. However, it can be shown that the three diffusion regimes are not spatially separated. The step sizes corresponding to these three diffusion modes are equally distributed over all parts of the track, not segregated in one or other of the domains A, B or C: the mobility of the molecule does not differ significantly from one domain to the other. Instead, owing to structural heterogeneities, the environment within one channel system changes strongly along the pathway of the molecule. These heterogeneities are revealed by the molecule continuously changing its mode of motion between at least three diffusion coefficients. Therefore, its diffusion cannot be described as a simple Brownian motion. An interpretation of these results could actually be a range of diffusion coefficients due to variations of local environment.

Hence, this example of trajectory analysis demonstrates that the diffusion coefficients vary not only between different phases (as shown in the previous Section) or between trajectories of individual molecules within one phase, but can also change within the same trajectory of an individual molecule.

5. Oriented Single Molecules with Switchable Mobility in Long Unidimensional Nanochannels

Using the surfactant CTAB (Cetyltriethylammoniumbromide) in the template synthesis of the mesoporous M41S systems instead of Brij56 (used for the fabrication of the films studied in Sections 2-4) we obtained hexagonally arranged channels where the diameter of the channel (2-3 nm) is smaller than the length of the TDI molecule (3.2 nm) used as fluorescent probe. Therefore rotation of the TDI molecule about its long axis should be impossible in well-ordered channels.

Polarization modulated confocal microscopy was performed to monitor simultaneously the diffusional and orientational behavior of the TDI molecules in such systems [4]. Fig. 5a shows three fluorescence images taken at time 0 min., 2 min. and 4 min. where single TDI dye molecules appear with a characteristic fluorescence-intensity profile (striped patterns) due to the polarization modulation during the scan. From these patterns we compute both the position of the molecule and the orientation of its transition dipole moment (shown by small bars). Following the molecule in the circle we can obtain the trajectory of this single TDI molecule including position and orientation as shown in Fig. 5b. The trajectory shows that the molecule is moving linearly back and forth over a distance of about 2 μm , while it remains remarkably aligned with the direction of the diffusion, which we assigned to the direction of the pores. Fig. 5c shows the alignment of the fluorophore with respect to the pores which clearly indicates that free rotation is prevented by the well-ordered channel and the geometrical constraints due to the size of the molecule and the diameter of the channel. Thus the orientation of single TDI molecules and their trajectories map directly the direction of the channels. Furthermore, the rotational free translation of the single molecule indicates a structurally well-ordered area.

We have developed a method with which we could improve the film preparation to produce highly ordered linear channels in domains up to 100 μm in size [4]. To our knowledge such a high degree of order over long distances has not been reported before for mesoporous structures. It is however, highly desirable for many applications. The observations shown in Fig. 5a-c were taken with the mesoporous film in a saturated chloroform atmosphere. In this case the molecules were mobile. Changing the atmosphere above the film with air (40 % relative humidity) the molecular motion immediately stopped. This process is highly reversible and indicates that by changing the atmosphere around the porous film the diffusion of TDI guest molecules can be easily switched on and off reversibly (Movies 1 and 2 in Supplementary Material of ref. [4]). These observations lead us to a model for the im-/mobility of the TDI molecules in the mesoporous host: The TDI molecule has a very hydrophobic core and four oxygen atoms pointing to the side (Fig. 5d-e) whose lone-pair electrons can interact with the positively charged heads of the CTAB molecules. In addition interactions are possible with active silanol groups or other defects in the channel walls. These interactions seem to be responsible for the immobilization of the molecule in air atmosphere (Fig. 5d). In contrast, when chloroform, a good solvent for TDI, is added to the system it is likely that the small solvent molecules form a lubricant-like phase inside the pores (Fig. 5e). As a result the TDI molecules can be solvated and diffuse along the pores [4]. Hence the solvent exchange allows an easy control of the diffusional behaviour of the guest molecules.

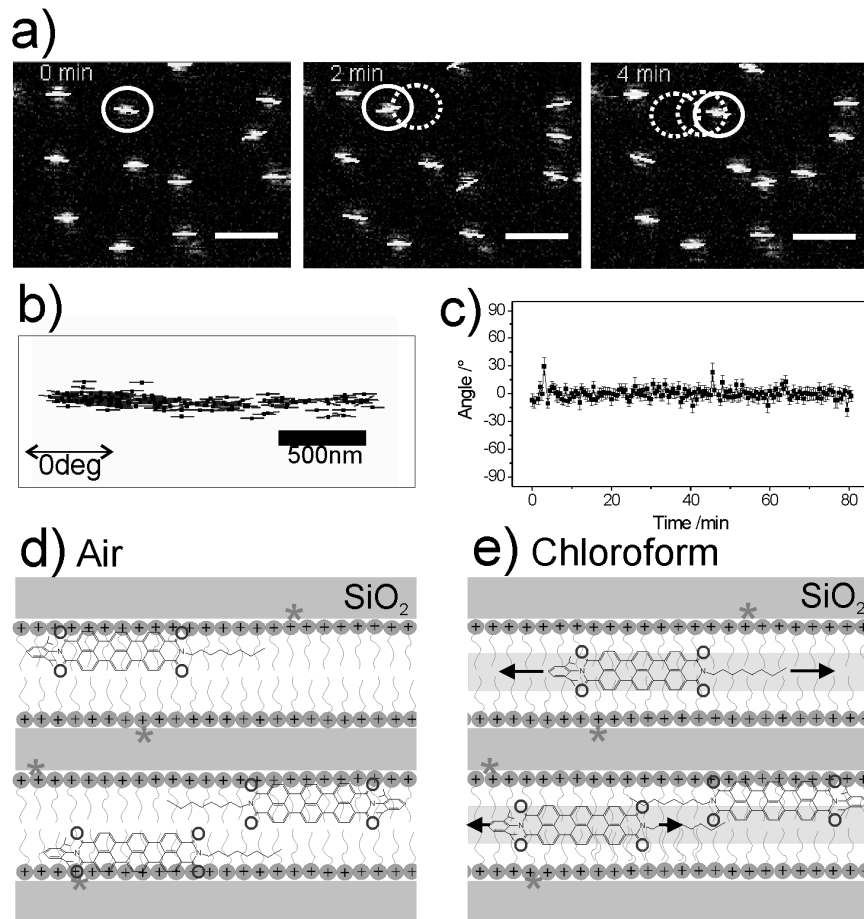


Fig. 5: **Parallel orientation and diffusion of single TDI molecules in a highly ordered domain.** a) Sequence of fluorescence images showing linear diffusion of single TDI molecules in a chloroform atmosphere extracted from a time series. Scale bar: 2 μm . b) Trajectory extracted from the molecule marked with the white circle in a). c) Calculated angular time trajectory of the same molecule. d) Sketch of TDI molecules immobilized in the mesoporous film in air atmosphere. The stars indicate active silanol groups. e) TDI molecules in the mesoporous film in the presence of chloroform. The solvent provides a lubricant for the molecular movement.

6. High Localization Accuracy of Single Molecules down to the Single Channel Limit

Our aim to achieve an extremely high positioning accuracy in the optical SMT experiments which is better than the pore diameter of the mesoporous system could be achieved in the CTAB templated M41S system [4]. Here the TDI molecules move slower than in the Brij56 templated system and by increasing the laser power and improving other parameters of the experiment we could achieve a spatial resolution of 2-3 nm. This allows us to identify a moving molecule in a specific channel and to observe jumps between neighbouring channels.

Fig. 6a shows the trajectory of a TDI molecule (Movie 6 in supplementary material of ref. [4]) which first moves in one channel (black trajectory) and then switches over into the neighbouring channel (grey trajectory). This can nicely be seen if we separate the movement along the pore and perpendicular to it in $x(t)$ and $y(t)$ graphs (Fig. 6c). By inspection of the $y(t)$ graph a jump to a neighbouring pore is observable after 103 s. Fig. 6b displays the histogram of $y(t)$ before (grey) and after (black) 103 s. The distributions are clearly distinct and can be fitted with two Gaussian curves with a maximum at 0.6 and 6.1 nm and with a half width of $\sigma = 2.9$ and $\sigma = 2.3$ nm respectively. We attribute the observed dynamics to a TDI molecule which is switching between two neighbouring pores separated by 5-6 nm as indicated in Fig. 6d. In other cases we observed molecules which explored even more distant pores by switching through defects from pore to pore. This seems to be an important process for a molecule to circumvent dead ends in one pore and to travel over larger distances within the mesoporous system. Fig. 6a is also an example for this behaviour because the molecule in the first channel is kept between two dead ends and can extend its pathway along the pores only by switching in the neighbouring channel.

The $x(t)$ graph of this molecule as shown in Fig. 6b reveals another interesting property: the trapping of a molecule during its passage through the channel network. Whenever the molecule reaches one of the two dead ends of the first channel it is trapped for some seconds. The same is true when it moves in the neighbouring channel. A detailed analysis of the trajectories of 80 molecules reveals a Gaussian distribution of the diffusion coefficients (Fig. 6e) with a mean value of $D = 3.9 \times 10^{-4} \mu\text{m}^2/\text{s}$ and a half width of $\delta = 10^{-4} \mu\text{m}^2/\text{s}$. In addition the histogram of the percentage of the adsorption time per trajectory (Fig. 6f) is also Gaussian with a maximum at 18 %. This means that a molecule spends on average 18 % of its walk immobilized at an adsorption site. Such kinetic data can give a very detailed picture of the dynamic behaviour of molecules inside the channel network of a mesoporous system.

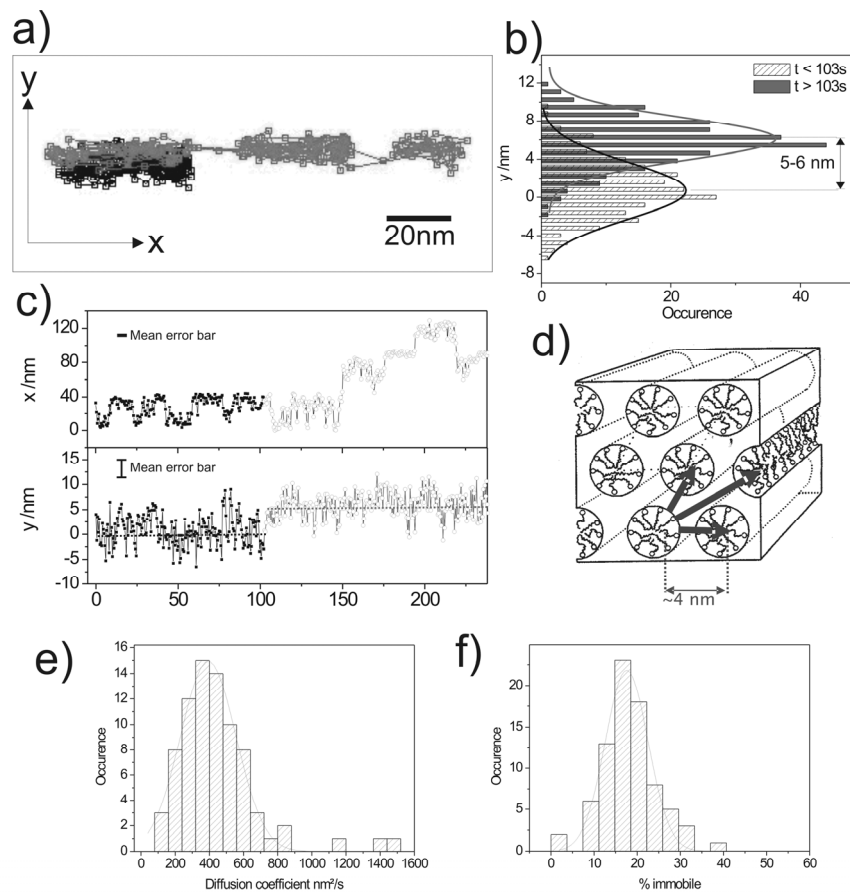


Fig. 6: Diffusion and switching in two distinct neighbouring channels and trapping behaviour. a) Trajectory with high optical resolution of a single TDI molecule switching from one channel (black) to a neighbouring channel (grey). b) Histogram with Gaussian distribution of the lateral (y) coordinate for the time intervals before (black) and after (grey) the switching to the neighbouring channel at time $t = 103$ s. c) Projected $x(t)$ and $y(t)$ coordinates for the single TDI molecule in a) diffusing in two distinct neighbouring pores. $y(t)$ clearly shows the switch into the neighbouring channel at the time $t = 103$ s. $x(t)$ shows repeatedly trapping of the single TDI molecule at the walls. d) Hexagonal channel system of the CTAB templated mesoporous host with arrows indicating a switch to neighbouring channels. e) Histogram of the diffusion coefficients of 80 molecules in a CTAB templated mesoporous film. f) Histogram of the percentage of adsorption time per trajectory of 80 molecules in the same system.

7. Functionalized Mesoporous Silica Structures - Towards Novel Drug Delivery Systems

For many applications, the mesoporous materials are expected to show enhanced properties when their inner channel walls are functionalized with organic moieties to fine-tune host-guest interactions. This is particularly important for drug delivery systems which require the drug to be released at a slow rate in order to generate the desired depot-effect.

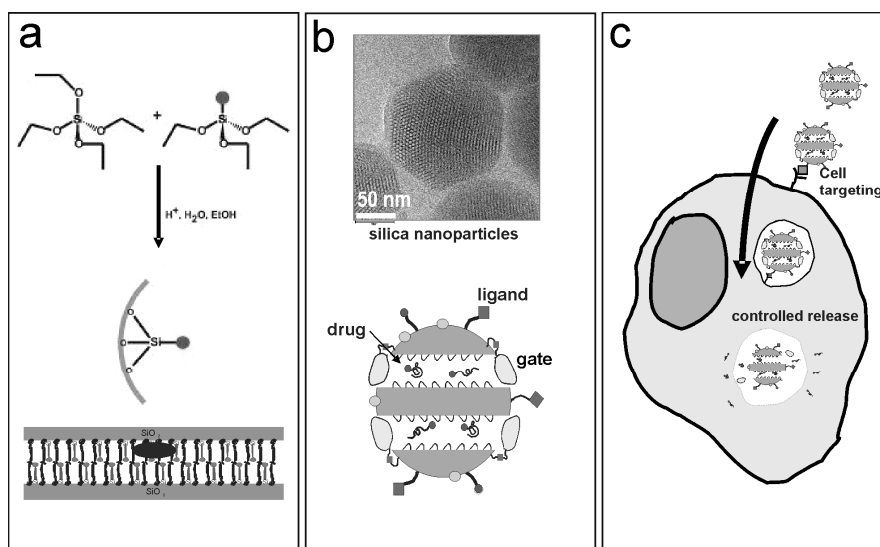


Fig. 7: **Mesoporous silica nanoparticles as novel drug delivery systems.** a) Co-condensation method to form functionalized mesoporous silica structures in a surfactant template synthesis. b) TEM image of mesoporous silica nanoparticles and sketch of a novel drug delivery particle which contains functionalized pores, closed by a gate, and is decorated with ligands for cell targeting. c) Cell targeting by ligand-receptor interaction at the cell membrane, endosomal uptake and controlled release after pH change from early to late endosome.

In our study a co-condensation method [23] was used to enable the homogeneous incorporation of functional groups (Fig. 7a) like e.g. alkyl chains or cyano-propyl groups which differ strongly in polarity. This resulted in a strong influence on the diffusion coefficient of the probe molecule [24].

Furthermore, mesoporous nanoparticles with a diameter of about 100 nm can be produced as shown in the upper part of Fig. 7b. We intend to use them as the basis for a novel drug delivery system which is sketched in the lower part of Fig. 7b. This system carries several functions for controlled release and targeting of specific cells. These functions are: i) functionalized pore walls to create a depot effect and controlled release of the drug; ii) a gate which closes the channels and can be opened by a pH drop from pH 7 to pH 5, taking place from an early to a late endosome within the cell; iii) ligands

attached to the nanoparticle which serve for cell targeting using specific receptors at the cell surface. The nanoparticle attaches with its ligand to a specific receptor at the cell membrane. Then it is endocytosed and the early endosome transforms into a late endosome by changing its pH from 7 to 5. This will open the gates of the nanoparticle and a controlled release of the drug can take place (Fig. 7c). Such novel drug delivery systems will be especially useful for the delivery of toxic drugs like e.g. cytostatica in cancer chemotherapy, where the drug delivery system is targeted to the cancer cell and opens its toxic load not before it is inside the cancer cell. This novel drug delivery system using mesoporous nanoparticles with different functionalities is presently under development in our laboratory.

8 Synthetic Viruses as Gene Delivery Systems

Synthetic viruses are drug delivery systems in which the drug is a therapeutic gene [25-27]. They are used in gene therapy [28]. There are two different ways to introduce a gene into the cell nucleus: with the help of viruses [29] (viral vectors) or by means of synthetic viruses [26, 27] (non-viral vectors). In general the viral vectors induce a high expression of the target gene. Nevertheless, their disadvantage is the immunogenic response of the body upon administration. For this reason, a lot of research has been done on alternative vectors like synthetic viruses, which, however, are not as efficient as natural viruses. They consist of plasmid DNA condensed by e.g. a cationic polymer forming a so-called polyplex [26, 27]. In order to induce gene expression, the DNA has to enter the cell nucleus. On its way to the cell nucleus there are several barriers to overcome like the cell membrane, the escape from the endosome and the nuclear membrane. These processes are shown in Fig. 8a. First the synthetic viruses have to enter the cell which can occur by different uptake processes like receptor induced endocytosis and others [30, 31]. Besides diffusion in the cell cytoplasm transport processes with motor proteins are responsible to bring the polyplex closer to the nucleus [32, 33]. In addition the complex has to escape the endosome [34, 35] and finally the DNA has to be transported into the nucleus. Viruses have developed specialized mechanisms to overcome the barriers and to be transported very efficiently. Non-viral vectors or synthetic viruses in contrast have to be programmed chemically using e.g. a biomimetic approach. This can be based on the experience resulting from investigations of the infection pathway of single viruses in living cells [36, 37]. In order to make synthetic viruses more efficient the uptake and transport processes have to be characterized in detail in order to identify bottlenecks in the internalization pathway. This can be done with optical single particle tracking techniques similar to the tracking of single molecules in nanoporous systems.

We used polyethylenimine (PEI) as polycation to bind nuclear acids and to form the synthetic viruses [32, 33]. In order to allow tissue selective delivery of these polyplexes, cell-specific ligands are attached to the polyplexes. To specifically target cancer cells, in which e.g. the epidermal growth factor (EGFR) is overexpressed by a factor of more than 100, the corresponding EGF ligand is used. Moreover, the plasmid DNA condensed in the polyplex is labelled with a fluorescent dye. This allows us to observe individual synthetic viruses by means of highly sensitive fluorescence wide-field microscopy during

different stages of their internalization process, starting with the initial binding to the cell membrane and followed by the internalization and intracellular transport.

Fig. 8b shows the trajectory of an individual synthetic virus during such an internalization process [33] (Movie: see supplementary material of ref. [33]). Three different phases can be identified: In phase I, binding to the plasma membrane is followed by a slow movement with drift, which can be deduced from the quadratic dependence of the mean square displacement $\langle r^2 \rangle$ as a function of time. Furthermore, a strong correlation between neighbouring particles is seen and subsequent internalization is observed and can be proven by quenching experiments. During this phase, the particles are subjected to actin-driven processes mediated by transmembrane proteins. Phase II is characterized by a sudden increase in particle velocity and random movement, often followed by confined movement.

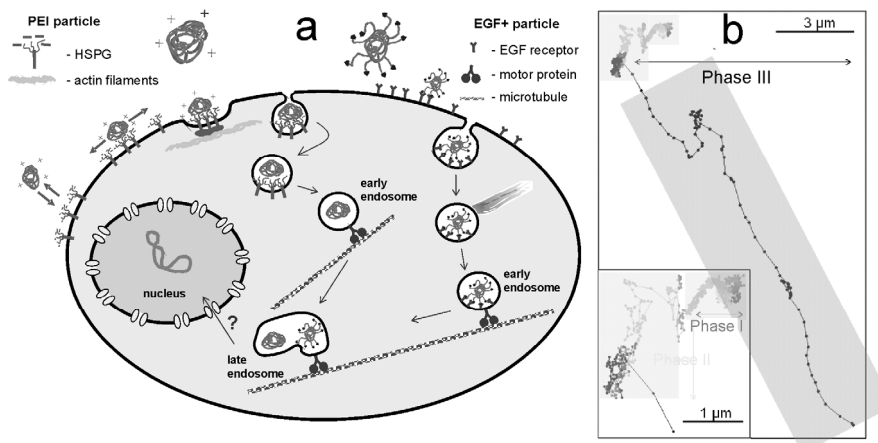


Fig. 8: **Uptake and trafficking of synthetic viruses in a cell.** a) Uptake and trafficking processes of plain (left) and EGF+ decorated (right) polyplexes in a cell shown in a schematic way. b) Trajectory of a single EGF+ polyplex showing three phases: phase I and phase III are directed movements whereas phase II is in most cases normal diffusion. Phase I and phase II are enlarged in the inset. The whole trajectory was recorded in 4.30 min at a frame rate of 300 ms.

This is indicated by a linear or saturating behaviour of $\langle r^2 \rangle$ as a function of time. In this phase the particles entrapped in intracellular vesicles are diffusing in the cytosol, waiting for an encounter with a motor protein as a microtubule-dependent transporting system. Phase III started with a dramatic increase in particle velocity and directed movement over long distances (several micrometer) within the cell along microtubules.

The directed movement is demonstrated by the quadratic dependence of $\langle r^2 \rangle$ as a function of time with transport velocities up to 4 $\mu\text{m/s}$.

As a result the internalization of EGF+ polyplexes in phase I was very rapid: 50% of the observed particles were internalized within 5 minutes. In sharp contrast, internalization of plain polyplexes which do not contain EGF was much slower and far less efficient. To our knowledge, this is the first study [35] describing the dynamics of targeted artificial viruses on a single-particle basis, in respect to cell binding and intracellular transport. From such results a very detailed knowledge can be obtained about the mechanistic processes of uptake and transport, which helps to improve the design and the functionality of synthetic viruses as a specific system for drug delivery.

Acknowledgements

We are very grateful to all co-workers and collaborators who are mentioned in our publications and who have shaped the understanding of molecular dynamics in nanoporous systems and drug delivery in living cells. The work was supported by the Excellence Clusters Nanosystems Initiative Munich (NIM) and Center for Integrated Protein Science Munich (CIPSM) as well as the collaborative research centers SFB 486 and SFB 749.

References

- [1] J. Kirstein, B. Platschek, C. Jung, R. Brown, T. Bein, C. Bräuchle, *Nature Materials* 6 (2007) 303-310.
- [2] A. Zürner, J. Kirstein, M. Döblinger, C. Bräuchle, T. Bein, *Nature* 450 (2007) 705-708.
- [3] C. Jung, C. Hellriegel, B. Platschek, D. Wöhrle, T. Bein, J. Michaelis, C. Bräuchle, *Journal of the American Chemical Society* 129 (2007) 5570-5579.
- [4] C. Jung, J. Kirstein, B. Platschek, T. Bein, M. Budde, I. Frank, K. Müllen, J. Michaelis, C. Bräuchle, *Journal of the American Chemical Society* 130 (2008) 1638-1648.
- [5] C. Jung, C. Hellriegel, J. Michaelis, C. Bräuchle, *Advanced Materials* 19 (2007) 956-959.
- [6] F. Feil, C. Jung, J. Kirstein, J. Michaelis, C. Li, F. Nolde, K. Müllen, C. Bräuchle, in *Press*, 2009, DOI: 10.1016/j.micromeso.2009.01.024.
- [7] D.E. De Vos, M. Dams, B.F. Sels, P.A. Jacobs, *Chemical Reviews* 102 (2002) 3615-3640.
- [8] V. Rebbin, R. Schmidt, M. Froba, *Angewandte Chemie-International Edition* 45 (2006) 5210-5214.
- [9] D.J. Cott, N. Petkov, M.A. Morris, B. Platschek, T. Bein, J.D. Holmes, *Journal of the American Chemical Society* 128 (2006) 3920-3921.
- [10] B. Ye, M.L. Trudeau, D.M. Antonelli, *Advanced Materials* 13 (2001) 561-565.
- [11] N. Petkov, N. Stock, T. Bein, *Journal of Physical Chemistry B* 109 (2005) 10737-10743.
- [12] I. Braun, G. Ihlein, F. Laeri, J.U. Nockel, G. Schulz-Ekloff, F. Schüth, U. Vietze, O. Weiss, D. Wöhrle, *Applied Physics B-Lasers and Optics* 70 (2000) 335-343.

- [13] I.O. Roy, Y. Tymish, D.J. Bharali, H.E. Pudavar, R.A. Mistretta, N. Kaur, P.N. Prasad, *PNAS* 102 (2005) 279-284.
- [14] C.J. Brinker, Y. Lu, A. Sellinger, H. Fan, *Adv. Mater.* 11 (1999) 579-585.
- [15] O. Terasaki, T. Ohsuna, in: Auerbach SM, Carrado KA, Dutta PK (eds) *Handbook of Zeolite Science and Technology*, Dekker, New York, 2003, 291-315.
- [16] V. Kukla, J. Kornatowski, D. Demuth, I. Girnus, H. Pfeifer, L.V.C. Rees, S. Schunk, K.K. Unger, J. Kärger, *Science* 272 (1996) 702-704.
- [17] N.E. Benes, H. Jovic, H. Verweij, *Microporous and Mesoporous Materials* 43 (2001) 147-152.
- [18] Y. Sakamoto, M. Kaneda, O. Terasaki, D.Y. Zhao, J.M. Kim, G. Stucky, H.J. Shin, R. Ryoo, *Nature* 408 (2000) 449-453.
- [19] C. Jung, B.K. Müller, D.C. Lamb, F. Nolde, K. Müllen, C. Bräuchle, *Journal of the American Chemical Society* 128 (2006) 5283-5291.
- [20] R.M. Dickson, D.J. Norris, W.E. Moerner, *Phys. Rev. Lett.* 81 (1998) 5322-5325.
- [21] C. Hellriegel, J. Kirstein, C. Bräuchle, V. Latour, T. Pigot, R. Olivier, S. Lacombe, R. Brown, V. Guieu, C. Payrastra, A. Izquierdo, P. Mocho, *Journal of Physical Chemistry B* 108 (2004) 14699-14709.
- [22] C. Hellriegel, J. Kirstein, C. Bräuchle, *New Journal of Physics* 7 (2005) 1-14.
- [23] W.S. Han, Y. Kang, S.J. Lee, H. Lee, Y. Do, Y.-A. Lee, J.H. Jung, *The Journal of Physical Chemistry B* 109 (2005) 20661-20664.
- [24] T. Lebold, L.A. Mühlstein, J. Blechinger, M. Riederer, H. Amenitsch, R. Köhn, K. Peneva, K. Müllen, J. Michaelis, C. Bräuchle, T. Bein, *Chem. Eur. J.* 15 (2009) 1661-1672.
- [25] S.M. Sullivan, in: Rolland A, (eds.) *Pharmaceutical Gene Delivery Systems*, Dekker, New York, 2003, 1-16.
- [26] T.G. Park, J.H. Jeong, S.W. Kim, *Advanced Drug Delivery Reviews* 58 (2006) 467-486.
- [27] D. Schaffert, E. Wagner, *Gene Therapy* 15 (2008) 1131-1138.
- [28] T.R. Flotte, *Journal of Cellular Physiology* 213 (2007) 301-305.
- [29] R. Waehler, S.J. Russell, D.T. Curiel, *Nat Rev Genet* 8 (2007) 573-587.
- [30] I. Kopatz, J.-S. Remy, J.-P. Behr, *The Journal of Gene Medicine* 6 (2004) 769-776.
- [31] J. Rejman, A. Bragonzi, M. Conese, *Mol Ther* 12 (2005) 468-474.
- [32] R. Bausinger, K. von Gersdorff, K. Braeckmans, M. Ogris, E. Wagner, C. Bräuchle, A. Zumbusch, *Angewandte Chemie International Edition* 45 (2006) 1568-1572.
- [33] K. de Bruin, N. Ruthardt, K. von Gersdorff, R. Bausinger, E. Wagner, M. Ogris, C. Bräuchle, *Molecular Therapy* 15 (2007) 1297-1305.
- [34] Y.W. Cho, J.-D. Kim, K. Park, *J. Pharm. Pharmacol.* 55 (2003) 721-734.
- [35] K.G. de Bruin, C. Fella, M. Ogris, E. Wagner, N. Ruthardt, C. Bräuchle, *Journal of Controlled Release* 130 (2008) 175-182.
- [36] G. Seisenberger, M.U. Ried, T. Endreß, H. Büning, M. Hallek, C. Bräuchle, *Science* 294 (2001) 1929-1932.
- [37] M. Lakadamyali, M.J. Rust, H.P. Babcock, X. Zhuang, *Proc. Natl. Acad. Sci.* 100 (2003) 9280-9285.